

## Supporting Information

### 1D/2D NiFeP/NiFe-OH heterostructure: roles of the unique nanostructure in stabilizing highly efficient oxygen evolution reaction

Fuzhen Zhao,<sup>[a]</sup> Xin Zheng,<sup>[b]</sup> Xinyu Mao,<sup>[a]</sup> Huicong Liu,<sup>[a]</sup> Liqun Zhu,<sup>[a]</sup> Weiping Li,<sup>[a]</sup> Hui Ye,<sup>\*</sup> <sup>[c]</sup>Haining Chen<sup>\*[a]</sup>

[a] School of Materials Science and Engineering, Beihang University, No. 37 Xueyuan Road, Haidian District, Beijing 100191, China

[b] State Key Laboratory of Heavy Oil Processing, China University of Petroleum, Beijing 102249, China

[c] Aerospace Research Institute of Materials and Processing Technology, No. 1 South Dahongmen Road, Beijing 100076, China

## Experimental section

### Preparation of materials

Ferrous Sulfate ( $\text{FeSO}_4 \cdot 7\text{H}_2\text{O}$ ), sodium citrate dihydrate ( $\text{Na}_3\text{C}_6\text{H}_5\text{O}_7 \cdot 2\text{H}_2\text{O}$ ), sodium sulfate ( $\text{Na}_2\text{SO}_4$ ), potassium hydroxide (KOH), boric acid ( $\text{H}_3\text{BO}_3$ ), potassium carbonate ( $\text{K}_2\text{CO}_3$ ) muriatic acid (HCl) and sulfuric acid ( $\text{H}_2\text{SO}_4$ ) were purchased from the Beijing Chemical Works (Beijing, China). Sodium hypophosphite ( $\text{NaH}_2\text{PO}_2$ ) were purchased from Innochem-Beijing. Nickel sulfate ( $\text{NiSO}_4 \cdot 6\text{H}_2\text{O}$ ) and sodium hydroxide (NaOH) were purchased from Shanghai Aladdin Bio-Chem Technology Co., LTD. Trisodium phosphate anhydrous ( $\text{Na}_3\text{PO}_4$ ) were purchased from Shanghai Macklin Bochemical Co., LTD. The nickel foam was purchased from the Tianyu factory of Shandong province.

### Preparation of clean Ni Foam

The process include: (1) The Ni foam were washed and degreased in the solution containing 10 g L<sup>-1</sup> NaOH, 5 g L<sup>-1</sup> Na<sub>2</sub>SO<sub>4</sub> and 15 g L<sup>-1</sup> Na<sub>3</sub>PO<sub>4</sub> for oil removal. (2) The oxide layer on the surface of the Ni foam was removed in the solution containing 10 g L<sup>-1</sup> HCl and 20 g L<sup>-1</sup> H<sub>2</sub>SO<sub>4</sub>.

### Electrodeposition of single NiFe-OH

A 50 ml electrolytic bath was used for electrodeposition at a temperature of 25 °C. An aqueous nitrate solution with 0.1 M total metal ions ( $\text{Ni}^{2+}$  and  $\text{Fe}^{2+}$ ) served as the electrolyte. The substrate was treated to a cathodic deposition at 20 mA cm<sup>-2</sup> for 600 s in a conventional synthesis.

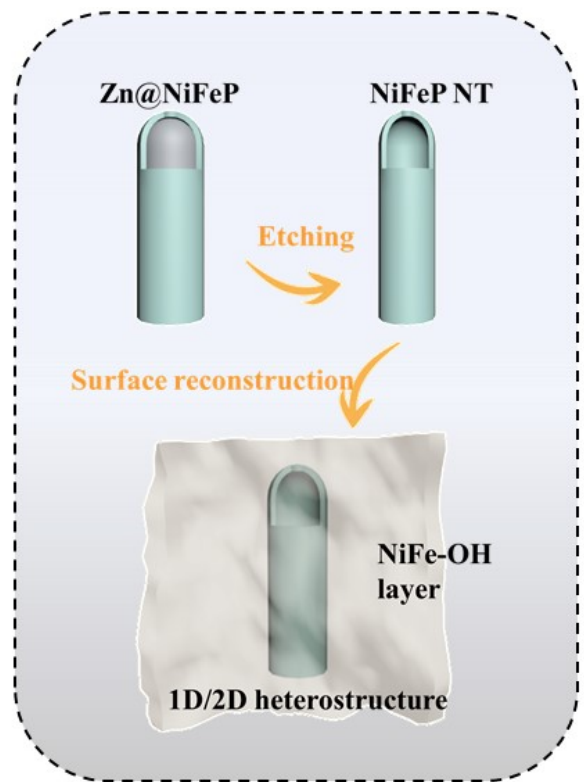


**Figure S1.** Schematic illustration of the synthesis processes.

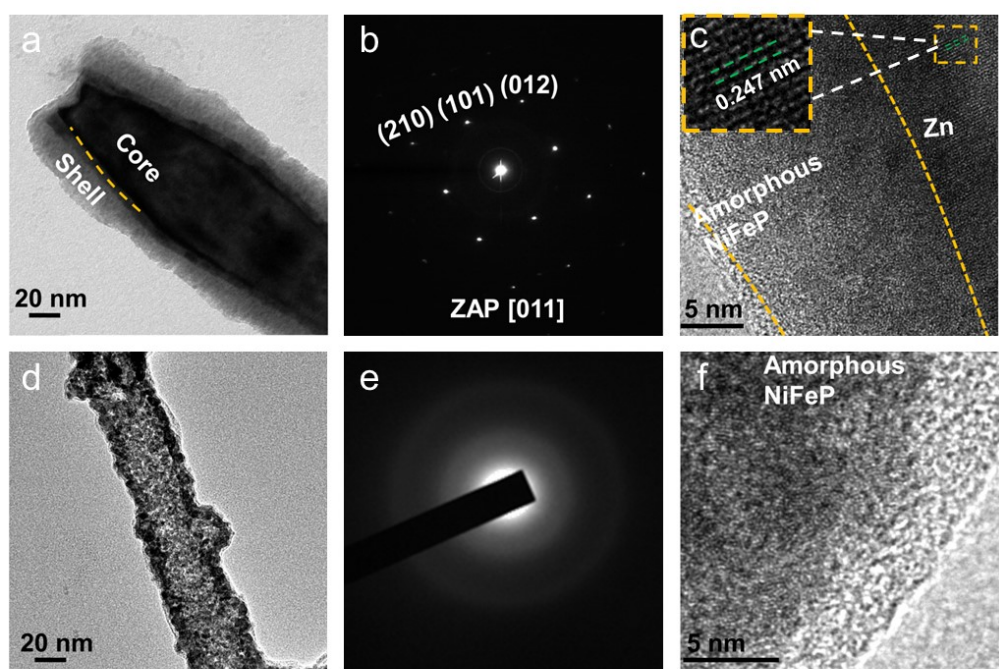


**Figure S2.** TEM results for the samples obtained at different steps. (a, d) TEM images, (b, e) SAED patterns, (c, f) HRTEM images of (a, b and c) Zn@NiFeP NWs and (d, e and f) 1D NTs.

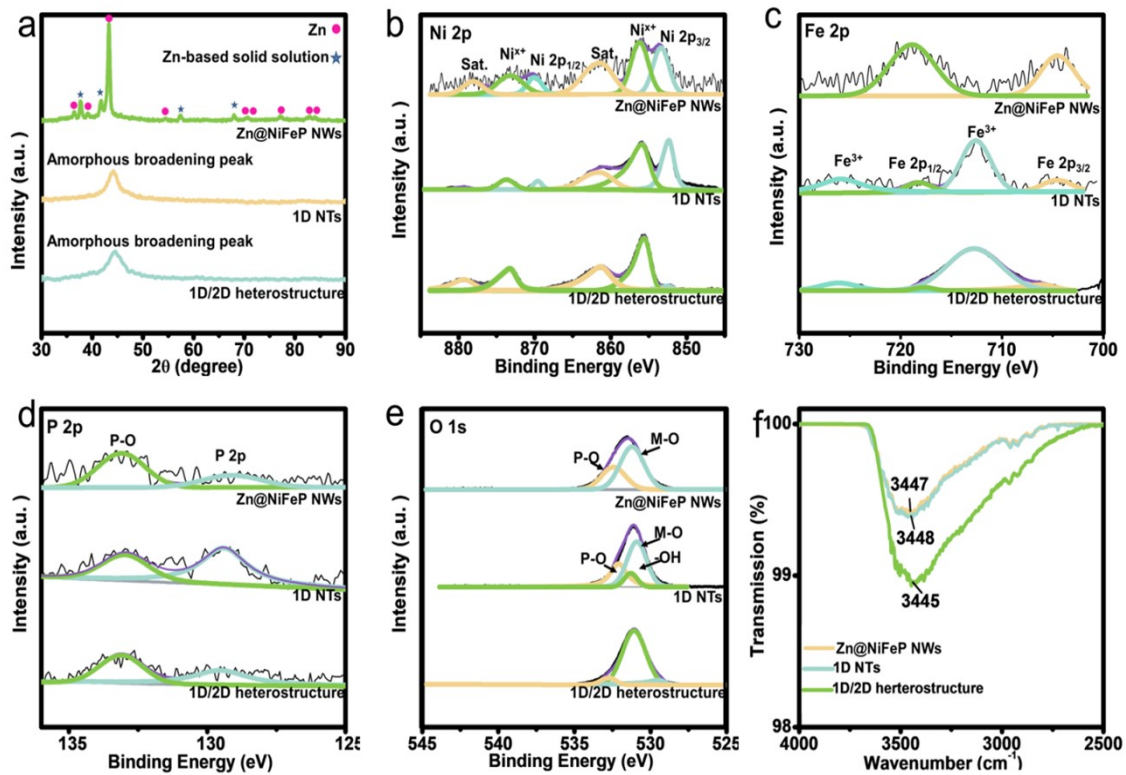


**Figure S3. Changes of structure and composition of the sample obtained at different steps.** (a) XRD patterns, (b) Ni 2p XPS spectra, (c) Fe 2p XPS spectra, (d) P 2p XPS spectra, (e) O 1s XPS spectra and (f) FTIR spectra of Zn@NiFeP NWs, 1D NTs and 1D/2D heterostructure.

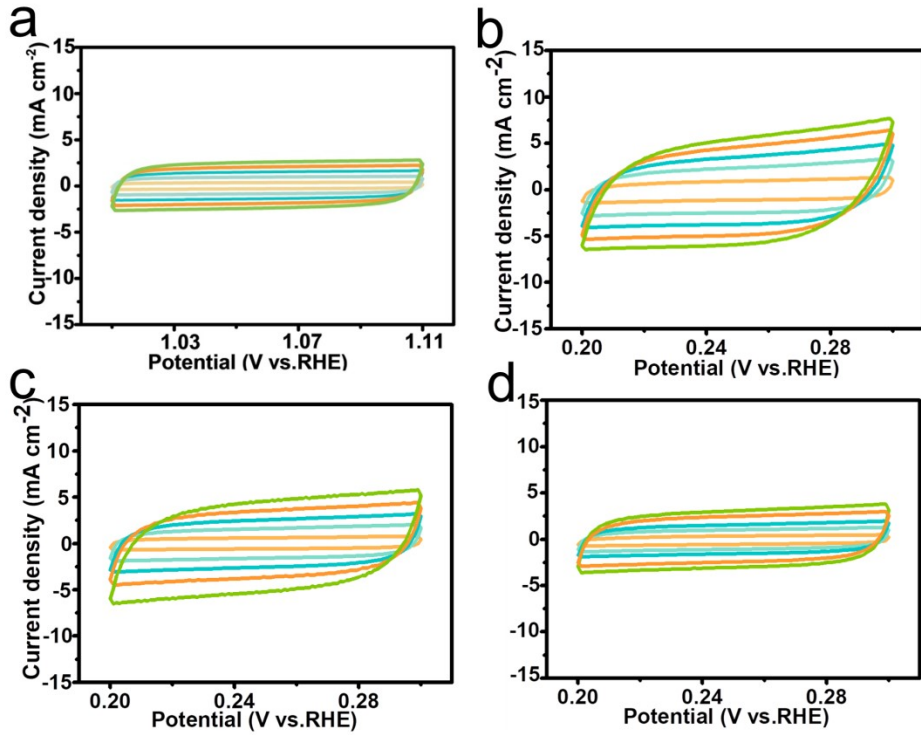


**Figure S4.** CV curves for ECSA measurements of  $\text{IrO}_2$  and 1D/2D heterostructure with different Fe content. (a)  $\text{IrO}_2$ . (b)  $\text{Ni:Fe}=96:4$ . (c)  $\text{Ni:Fe}=82:18$ . (d)  $\text{Ni:Fe}=64:36$ .

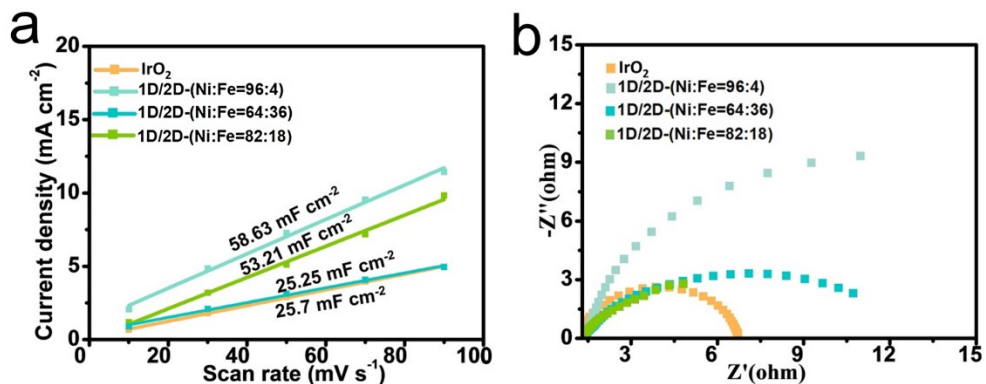


**Figure S5.** (a) Tafel plots of 1D/2D heterostructure with different Fe content. (b) EIS spectra of 1D/2D heterostructure with different Fe content

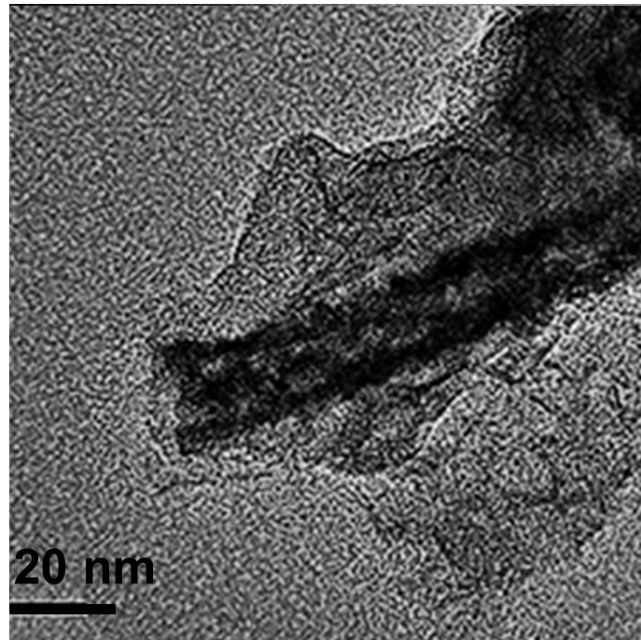


**Figure S6.** TEM image of 1D/2D heterostructure after 220 h OER measurement.

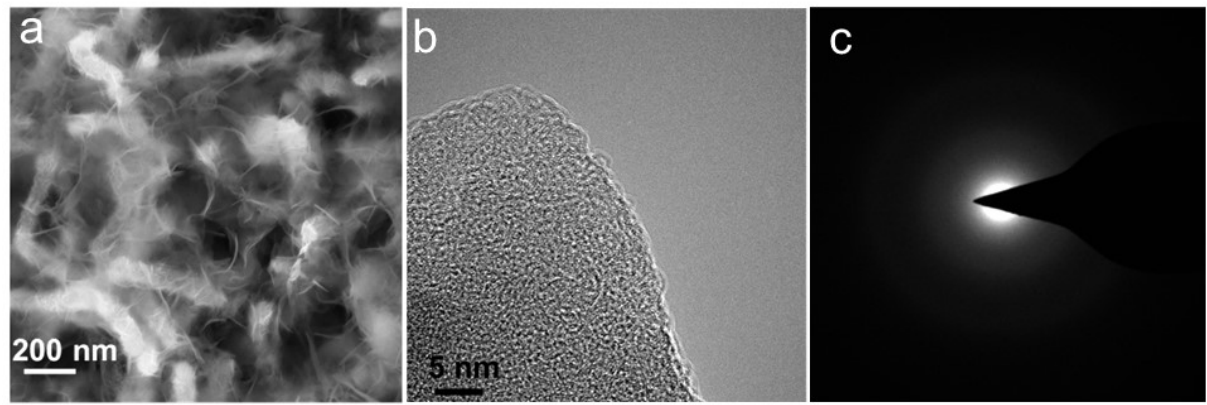


**Figure S7.** (a) SEM image, (b) HRTEM image and (c) SAED pattern of 1D/2D heterostructure after 220 h stability measurement.

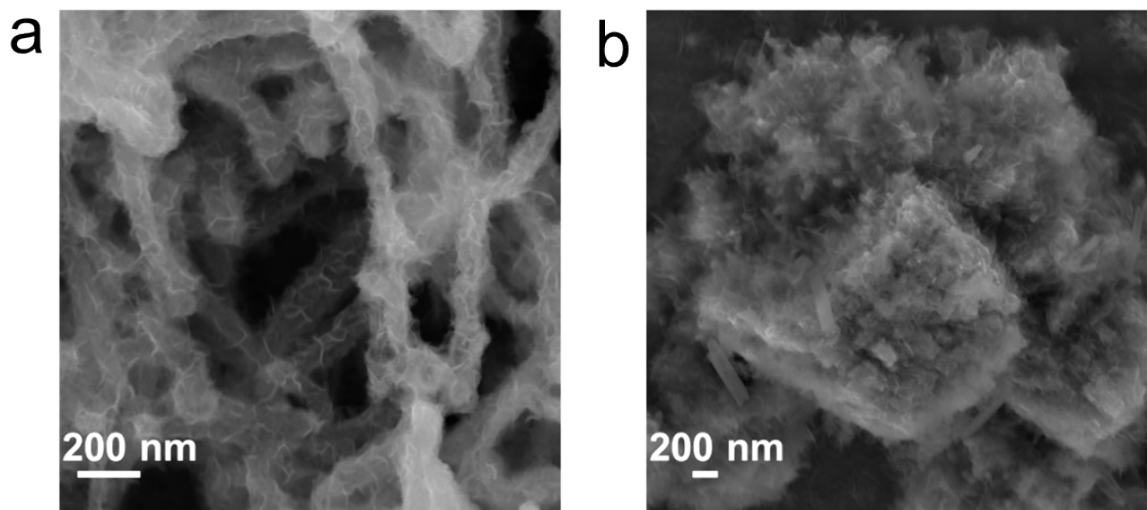


**Figure S8.** SEM images of sample with 4% Fe (a) and 36% Fe (b).

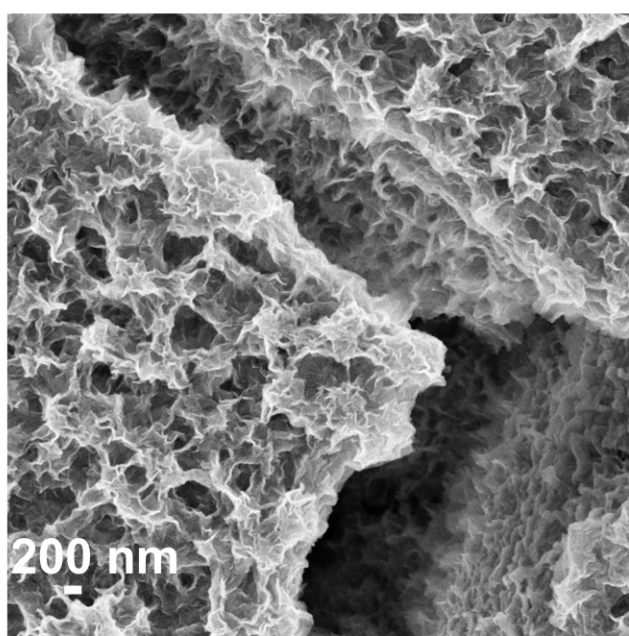


**Figure S9.** SEM image of measured single NiFe-OH.

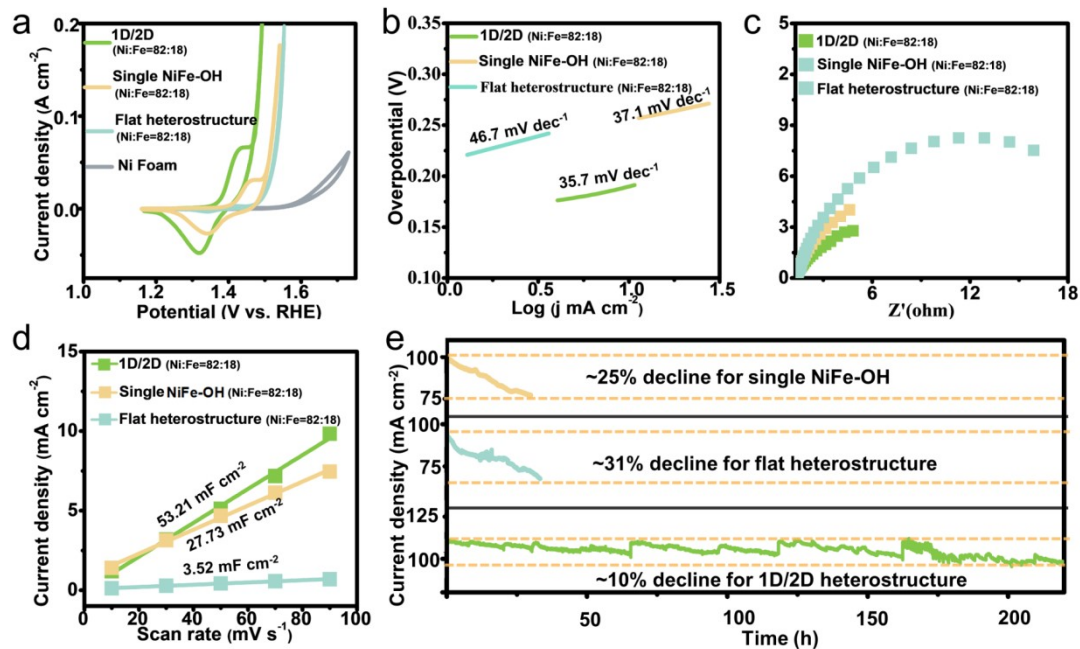


**Figure S10. Electrochemical measurements.** (a) CV curves, (b) Tafel slopes, (c) EIS spectra, (d) electrochemical double layer capacitance results for ECSA and (e) i-t curves of 1D/2D heterostructure, single NiFe-OH and flat heterostructure.

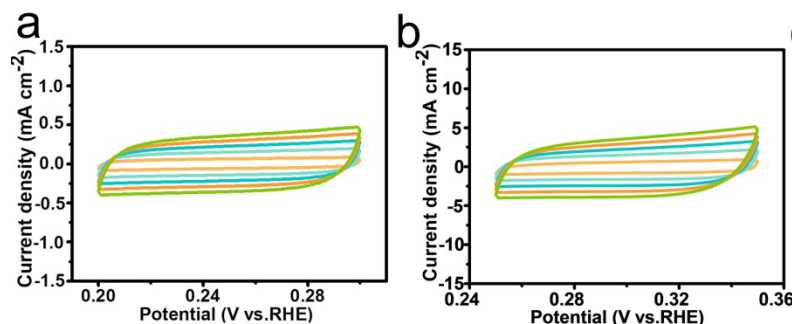


**Figure S11.** CV curves for ECSA measurements of (a) flat heterostructure and (b) single NiFe-OH.

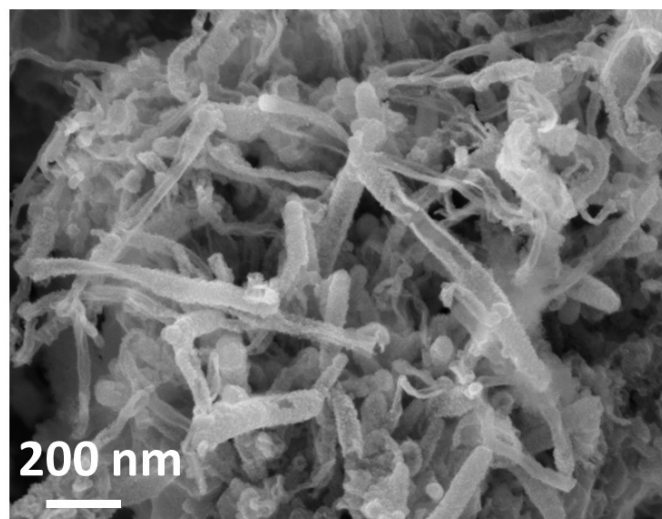


**Figure S12.** SEM image of measured 1D/2D heterostructure (220 h) after surface etching.

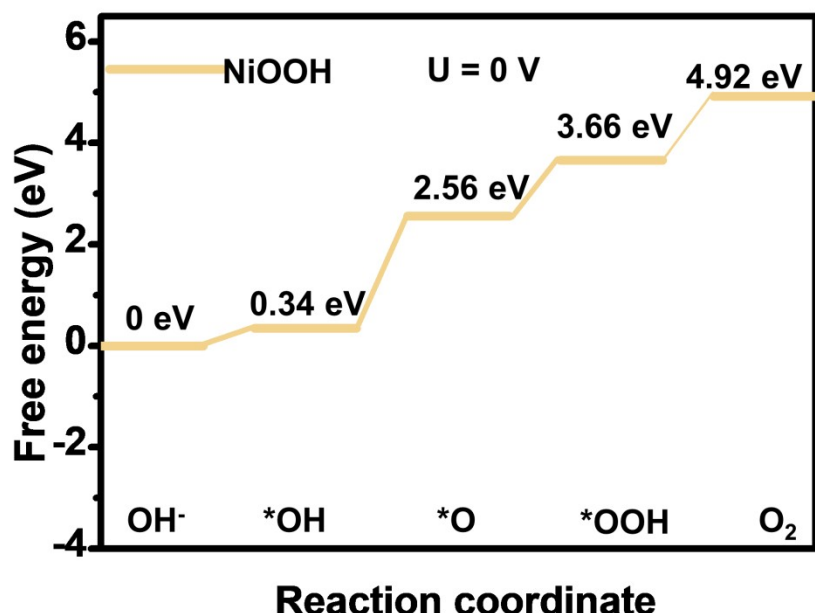


**Figure S13.** TEM image of 1D/2D heterostructure after 220 h OER measurement.

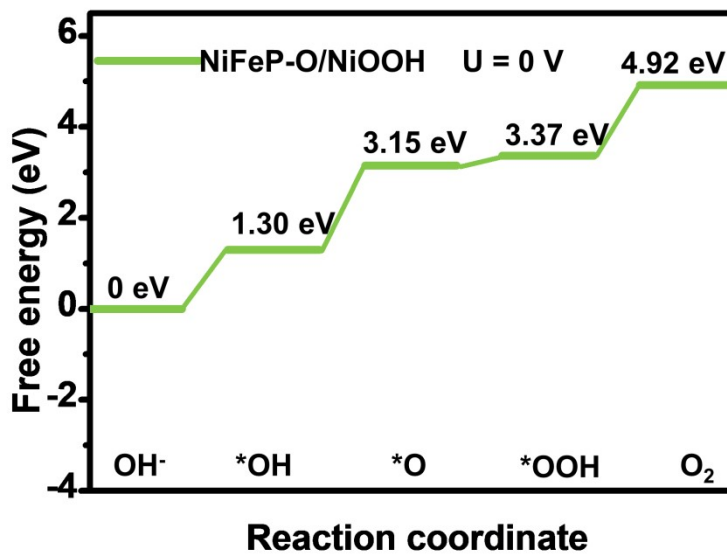


**Figure S14.** The calculated Gibbs free energy of NiFeP-O/NiOOH.

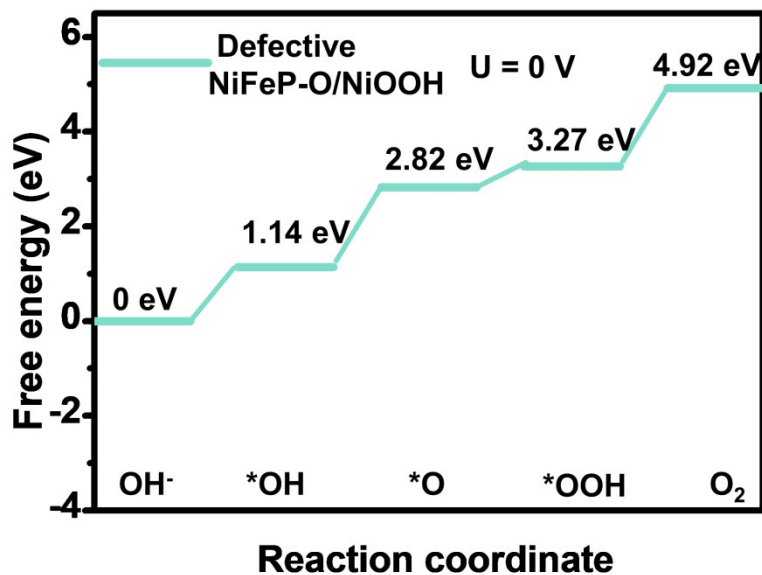


**Figure S15.** The calculated Gibbs free energy of defective NiFeP-O/NiOOH.

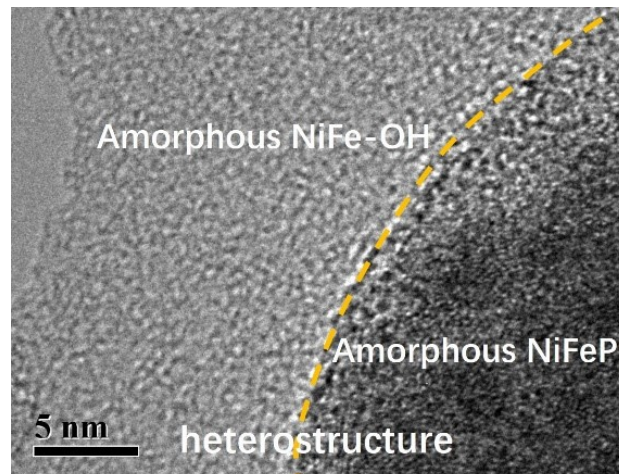


**Figure S16.** HRTEM image of 1D/2D heterostructure

**Table S1. The results of EDS mapping**

Zn@NiFeP NWs	NiFeP NTs	1D/2D		1D/2D		1D/2D	
		heterostructure	heterostructure after 220 h	heterostructure (low content of Fe)	heterostructure (low content of Fe)	1D/2D	
Atomic percent (%)	Atomic percent (%)	Atomic percent (%)	Atomic percent (%)	Atomic percent (%)	Atomic percent (%)	Atomic percent (%)	Atomic percent (%)
P	5.45	9.14	10.6	8.90	7.10	6.09	
Fe	5.38	14.03	16.29	12.60	3.60	29.94	
Ni	19.23	76.83	73.11	78.50	89.30	62.97	
Zn	69.94	-	-	-	-	-	

**Table S2.** Activity and stability of various reported NiFe-LDH and related NiFe hydroxide catalysts for OER in 1M KOH.

OER electrocatalysts	$\eta_{10}(\text{mV})$	Dur(h)	References
This work	190	220	
NiFe LDH@defective	210	10	1
NiFe LDH-rGO	250	9	2
NiFe LDH@HPGG	265	50	3
NiFe LDH @NGH	290	12	4
NiFe LDH QD@GH	220	10	5
NiFe LDH /C	210	28	6
NiFeCr LDH@CP	225	6	7
NiFeCe LDH-CNT	227	8.3	8
S–NiCoFe LDH NA	206	30	9
NiFe LDH@Cu NA	199	48	10
NiFe LDH-Cu <sub>3</sub> P NA	235	11	11
Ni NP-NiFe LDH	328	18	12
NiFe LDH@NiCoP NA	220	100	13
NiFe LDH@Ni <sub>3</sub> S <sub>2</sub>	190	40	14
NiFe <sub>2</sub> O <sub>4</sub> /NiFe LDH	213	20	15
NiFe LDH@Co <sub>3</sub> O <sub>4</sub>	269	40	16
FeOOH/NiFe LDH NA	207	20	17
Fe–Ni(OH) <sub>2</sub>	270	40	18
Ni/NiFe(OH) <sub>x</sub> NA	240	38	19
NiFe–Cu <sub>2</sub> O NA	215	50	20
R–NiFeOOH	270	11	21

**Table S3.** Calculation results of ZPE-TS for Gibbs free energy.

	H <sub>2</sub> O	H <sub>2</sub>	sur-OH*	sur-O*	sur-OOH*
ZPE - TS (eV)	0.084	0.05	0.34	0.08	0.28

**Table S4.** Thermodynamic data used in the calculations of Gibbs free energy

	E(eV)	G
H <sub>2</sub> O	-14.218518	-14.134807
H <sub>2</sub>	-6.77	-6.817005
O <sub>2</sub>	—	-9.71559
OH <sup>-</sup>	—	-10.726305
NiFeP-O/NiOOH	-654.77046	-683.04
NiFeP-O/NiOOH-OH*	-664.54105	-681.744
NiFeP-O/NiOOH-O*	-659.01612	-679.888
NiFeP-O/NiOOH-OOH*	-669.72842	-679.674
NiOOH	-387.82304	-416.093
NiOOH-OH*	-398.54586	-415.749
NiOOH-O*	-392.65726	-413.529
NiOOH-OOH*	-402.48702	-412.433
Defective NiFeP-O/NiOOH	-618.90051	-647.170
Defective NiFeP-O/NiOOH-OH*	-623.47677	-646.036
Defective NiFeP-O/NiOOH-O*	-633.96012	-644.349
Defective NiFeP-O/NiOOH-OOH*	-628.83232	-643.906

**References**

1. Y. Jia, L. Zhang, G. Gao, H. Chen, B. Wang, J. Zhou, M. T. Soo, M. Hong, X. Yan, G. Qian, J. Zou, A. Du and X. Yao, *Adv. Mater.*, 2017, **29**, 1700017.
2. T. Zhan, Y. Zhang, X. Liu, S. Lu and W. Hou, *J. Power Sources*, 2016, **333**, 53-60.
3. Y. Ni, L. Yao, Y. Wang, B. Liu, M. Cao and C. Hu, *Nanoscale*, 2017, **9**, 11596-11604.
4. R. Li, J. Xu, J. Ba, Y. Li, C. Liang and T. Tang, *Int. J. Hydrogen Energy*, 2018, **43**, 7956-7963.
5. J. Guo, X. Li, Y. Sun, Q. Liu, Z. Quan and X. Zhang, *J. Solid State Chem.*, 2018, **262**, 181-185.
6. S. Yin, W. Tu, Y. Sheng, Y. Du, M. Kraft, A. Borgna and R. Xu, *Adv. Mater.*, 2018, **30**, 1705106.
7. Y. Yang, L. Dang, M. J. Shearer, H. Sheng, W. Li, J. Chen, P. Xiao, Y. Zhang, R. J. Hamers and S. Jin, *Advanced Energy Materials*, 2018, **8**, 1703189.
8. H. Xu, B. Wang, C. Shan, P. Xi, W. Liu and Y. Tang, *ACS Applied Materials & Interfaces*, 2018, **10**, 6336-6345.
9. L.-M. Cao, J.-W. Wang, D.-C. Zhong and T.-B. Lu, *Journal of Materials Chemistry A*, 2018, **6**, 3224-3230.
10. L. Yu, H. Zhou, J. Sun, F. Qin, F. Yu, J. Bao, Y. Yu, S. Chen and Z. Ren, *Energy & Environmental Science*, 2017, **10**, 1820-1827.
11. P. Zhao, H. Nie, Z. Zhou, J. Wang and G. Cheng, *ChemistrySelect*, 2018, **3**, 8064-8069.
12. X. Gao, X. Long, H. Yu, X. Pan and Z. Yi, *J. Electrochem. Soc.*, 2017, **164**, H307.
13. H. Zhang, X. Li, A. Hähnle, V. Naumann, C. Lin, S. Azimi, S. L. Schweizer, A. W. Maijenburg and R. B. Wehrspohn, *Adv. Funct. Mater.*, 2018, **28**, 1706847.
14. G. Zhang, J. Yuan, Y. Liu, W. Lu, N. Fu, W. Li and H. Huang, *Journal of Materials Chemistry A*, 2018, **6**, 10253-10263.
15. Z. Wu, Z. Zou, J. Huang and F. Gao, *ACS Applied Materials & Interfaces*, 2018, **10**, 26283-26292.
16. S. Wang, J. Wu, J. Yin, Q. Hu, D. Geng and L.-M. Liu, *ChemElectroChem*, 2018, **5**, 1357-1363.
17. J. Chi, H. Yu, B. Qin, L. Fu, J. Jia, B. Yi and Z. Shao, *ACS Applied Materials & Interfaces*, 2017, **9**, 464-471.
18. J.-T. Ren, G.-G. Yuan, C.-C. Weng, L. Chen and Z.-Y. Yuan, *Nanoscale*, 2018, **10**, 10620-10628.
19. S. Zhuang, L. Wang, H. Hu, Y. Tang, Y. Chen, Y. Sun, H. Mo, X. Yang, P. Wan and Z. U. H. Khan, *ChemElectroChem*, 2018, **5**, 2577-2583.
20. H. Chen, Y. Gao and L. Sun, *ChemSusChem*, 2017, **10**, 1475-1481.
21. M. Asnavandi, Y. Yin, Y. Li, C. Sun and C. Zhao, *ACS Energy Letters*, 2018, **3**, 1515-1520.